

Published in final edited form as:

Cancer Res. 2009 September 1; 69(17): 7062–7070. doi:10.1158/0008-5472.CAN-09-0476.

Kisspeptin-10, a KISS1-Derived Decapeptide, Inhibits Tumor Angiogenesis by Suppressing Sp1-mediated VEGF Expression and FAK/Rho GTPase Activation

Sung-Gook Cho^{1,3,¶}, Zhengfang Yi^{1,2,¶}, Xiufeng Pang^{1,2}, Tingfang Yi², Ying Wang¹, Jian Luo², Zirong Wu², Dali Li², and Mingyao Liu^{1,2,3,*}

¹Center for Cancer and Stem Cell Biology, Institute of Biosciences and Technology and Department of Molecular and Cellular Medicine, Texas A&M University Health Science Center, Houston, Texas 77030, USA

²Institute of Biomedical Sciences and School of Life Sciences, East China Normal University, 500 Dongchuan Road, Shanghai 200241, China

³Interdisciplinary Genetics Program, Texas A&M University, College Station, TX77843

Abstract

Kisspeptin-10 (Kp-10), a decapeptide derived from the primary translation product of KISS1 gene, has been previously reported to be a key hormone for puberty and an inhibitor for tumor metastasis via the activation of G protein-coupled receptor 54 (Gpr54). However, whether Kp-10 inhibits angiogenesis, which is critical for tumor growth and metastasis and other human diseases, is still unknown. Here we demonstrate that Kp-10 significantly inhibits human umbilical vein endothelial cell (HUEVC) migration, invasion, and tube formation, key processes in angiogenesis. Using chicken chorioallantoic membrane (CAM) assay and VEGF-induced mouse corneal micropocket assay, we demonstrate that Kp-10 inhibits angiogenesis *in vivo*. Furthermore, Kp-10 inhibits tumor growth in SCID mice xenografted with human prostate cancer cells (PC-3) through inhibiting tumor angiogenesis while Kp-10 has little effect on the proliferation of HUVECs and human prostate cancer cells. In deciphering the underlying molecular mechanisms, we demonstrate that Kp-10 suppresses VEGF expression by inhibiting the binding of Sp1 to VEGF promoter and by blocking the activation of c-Src/FAK and Rac/Cdc42 signaling pathway in HUVECs, leading to the inhibition of tumor angiogenesis.

Keywords

KISS-1; GPR54; tumor angiogenesis; Kp-10; FAK; Rac1/Cdc42

Introduction

Angiogenesis, the growth of new blood vessels from pre-existing vessels, is crucial for tumor growth and metastasis (1). Numerous previous reports showed that it is effective to inhibit tumor growth and metastasis by blocking tumor angiogenesis (2). Angiogenesis is a complex process including endothelial cell proliferation, migration and tube formation. Vascular endothelial growth factor (VEGF), secreted from tumor cells and endothelial cells through either autocrine or paracrine manner, is critical for all steps of tumor progression,

*To whom correspondence should be addressed: Mingyao Liu, Ph.D., Institute of Biosciences and Technology, Texas A&M University Health Science Center, Houston, Texas 77030, 713-677-7505 (Phone), 713-677-7512 (Fax), mliu@ibt.tamhsc.edu.

¶These authors contributed equally to the work.

including tumor cell growth and angiogenesis (3–5). VEGF expression is regulated either by hypoxia-dependent or –independent pathways. The high GC-rich motifs in the proximal regions of VEGF promoter are regulated by transcriptional factor specificity protein 1 (Sp1) (6, 7), suggesting that Sp1 is implicated for the basal VEGF expression level in cells (8–11). When VEGF secreted by tumor cells interacts with VEGFR-2 in endothelial cells, VEGFR-2-binding c-Src recruits and fully activates FAK, which in turn stimulates downstream proteins such as Rho GTPases or MAPKs. Therefore, a decrease in VEGF expression or inhibition of VEGF-mediated signaling pathways in endothelial cells is important for the inhibition of tumor angiogenesis (12).

Human KISS1 gene encodes a premature 145-amino-acid protein which is proteolytically cleaved into polypeptides known as kisspeptins, including Kp-54 (also called metastin), Kp-14, Kp-13 and Kp-10 (13–15). Kisspeptins were originally identified as a metastasis suppressor in melanoma cells via binding and activating their cognate receptor GPR54 (14, 16–18). Further studies showed that loss of KISS1 gene expression was correlated with increased metastasis and/or tumor progression in a wide variety of tumor types, including malignant pheochromocytoma, esophageal squamous cell carcinoma, bladder tumor, ovarian, gastric, and pancreatic tumors (19–29). On the other hand, an increase in KISS1 and GPR54 expression with high grade and metastatic capacity has been reported in breast tumors and hepatocellular carcinomas (30–32). Recently, increased interests of Kisspeptins focused on their key roles in the regulation of the hypothalamic-pituitary-gonadal axis during puberty and reproductive development (11, 33–38). Among different kisspeptins, Kp-10 is the shortest peptide and highly conserved between mouse and human with one conserved amino acid replacement (18). Previous studies reported that Kp-10 regulated pubertal signaling in hypothalamus (38, 39), inhibited cell migration of primary human trophoblasts in placenta, suppressed metastatic activity of tumor cells (40), and acted as a vasoconstrictor (41). However, it is still unclear whether human Kp-10 inhibits angiogenesis or tumor angiogenesis. In this study, we investigated the effects of human Kp-10 on tumor angiogenesis and the underlying molecular mechanisms. We found that Kp-10 inhibited endothelial cell migration, invasion, and tube formation. Using chicken embryo chorioallantoic membrane (CAM) assay and mouse corneal micropocket models, we demonstrate that Kp-10 inhibits angiogenesis *in vivo*. Furthermore, Kp-10 inhibited tumor growth by suppressing tumor angiogenesis in xenograft mouse models with human prostate cancer cells. To understand the molecular mechanism of Kp-10 in regulating angiogenesis, we demonstrated that Kp-10 inhibited Sp1-mediated VEGF expression in tumor cells and suppressed the endothelial cell migration by blocking the activation of c-Src/FAK, Rac/Cdc42 GTPase. Therefore, our data suggest that Kp-10 inhibits angiogenesis and tumor growth by blocking Sp1-mediated VEGF expression and suppressing c-Src/FAK signaling pathway activation.

Materials and Methods

Cells, Cell Culture, Reagents, and Animals

PC-3, 293T cells were obtained from the American Type Tissue Collection and maintained in DMEM supplemented with 10% FBS and 1% antibiotics. Human Umbilical Vein Endothelial Cell (HUVEC) were kindly gifted from Dr. Xingli Wang (Cardiothoracic Surgery Division of the Michael E. DeBakey Department of Surgery at Baylor College of Medicine Hospital) and cultured in ECGM medium supplemented with 20% FBS, 1% BBE/Heparin mixture, 1% antibiotics, and 0.5% fungizone (1). VEGF was from R&D System provided by Biological Resources Branch, NCI-Frederick Cancer Research and Development Center. Matrigel was from BD Biosciences (San Jose, CA). Kp-10 peptide (purity>95%) was obtained from H.D Biosciences Co. Ltd (Shanghai, China) or Genenmed Synthesis, Inc. (South San Francisco, CA, US).

Fertilized chicken eggs were purchased from Shanghai Poultry Breeding Co. Ltd. C57BL/6 mice were from National Rodent Laboratory Animal Resources, Shanghai Branch in China. Severe combined immunodeficiency mice (SCID/Ncr) were purchased from National Cancer Institute.

Proliferation assay

Proliferation studies were carried out using the CellTiter96 AQueous One solution cell proliferation assay as previously described (1). Briefly, cells were plated at about 5000 HUVECs or PC-3 cells/well in 96-well plate and allowed to adhere to the plate with different concentration Kp-10. The cells were incubated for 48–72 hours and then the AQueous One solution (Promega, Madison, MI) was added to the samples and measured at 490nm.

Migration and tube formation assays

Two types of cell migration assays were performed using HUVEC cells. First, we examined cell migration in scratch assays as described previously (42). Cells cultured in 6 well culture dishes were scratched, washed with PBS and cultured for 24hr. Cells migrated toward the wound regions were imaged and counted. Then, modified Boyden chamber migration assays were performed as described previously (1), 4×10^4 HUVECs were cultured onto gelatin-coated 8 μm pore size chambers (BD Bioscience, San Jose, CA) and the bottom well was filled with 10ng/ μL VEGF as the chemoattractant. 24hr after incubating chambers, cells were fixed with 4% formaldehyde and stained with hematoxylin and eosin. Migrated cells were imaged and counted using Olympus IX70 invert microscope (Olympus) connected to digital camera DXM1200. For tube formation assay, 4×10^4 cells were cultured onto Matrigel-precoated 24 well culture dishes for 4hr at 37°C and were determined as counting branching points and tubes. Each experiment was performed four times, and independently done in triplicate.

Chicken Embryo Chorioallantoic Membrane Assay

According to previous method (43), embryonic eggs were incubated in 38.5–39°C with the relative humidity at 65–70%. Five days later, a 1–2cm² window was opened. The shell membrane was removed to expose the chorioallantoic membrane (CAM). As the carrier, 6mm-diameter Whatman filter disk which absorbed Kp-10 peptide was put on the CAM. Only PBS in the carrier was the control group. Then the window was sealed and eggs were incubated again. Four days later, the CAM was observed under stereomicroscope and the neovascularization was quantified. Assays for each test sample were carried out three times (n= 15~20).

Mouse Corneal Micropocket Assays

The mouse corneal assay was performed according to previously described (44). Corneal micropockets were created with a modified von Graefe cataract knife in one eye of each 5 to 6-week C57BL/6 mice. Micropellets (0.35×0.35 mm) of sucrose octasulfate-aluminum complex coated with hydron polyhydroxyethylmethacrylate containing 160ng of VEGF165 or 1 μg of Kp-10 plus 160ng of VEGF-165 were implanted into mouse corneal micropockets (n=10~11). Seven days later, photos and data were obtained. The area of neovascular response, vessel length and clock hours of new blood vessel were calculated according to the formula $\text{Area (mm}^2\text{)} = 0.2 \times \pi \times \text{VL (mm)} \times \text{CN (mm)}$, here CN is the clock hours of neovascularization, 1 clock hour equals 30 degrees of arc, VL = the maximal vessel length extending from the limbal vasculature toward the pellet.

Xenograft Tumor Growth Assay and Immunohistochemistry

3×10^6 PC-3 human prostate tumor cells were implanted subcutaneously on the back of 4-week-old male SCID mice ($n=6$). After tumor volume reaching 50mm^3 , Kp-10 ($50\ \mu\text{g}/50\ \mu\text{l}$ /mouse) was injected intraslesionally every day. Control groups were injected only with PBS. The growth of the tumor xenograft was evaluated in a pilot study by determining the tumor volume using digital caliper every 2 days. Tumor growth was measured as a following equation: $\text{length} \times \text{width}^2 \times 0.52$. Mice were continually observed until were killed. Tumors were removed and fixed and embedded with paraffin. Specific blood vessel staining was performed on the $5\ \mu\text{m}$ sections with CD31 antibody (1). Images were taken with ZEISS microscope. The number of blood vessels was counted.

Luciferase, EMSA, ChIP assays, and RT-PCR

HUVEC was transfected with pVEGF₂₀₁₈-luc, pVEGF₁₃₃-luc, or pVEGF₈₅-luc for 24hr and then subjected to the luciferase activity. For the luciferase assay, luciferase assay kit was used according to the manufacture's protocol (Promega, Madison, MI). Electrophoretic mobility shift assays (EMSA) were carried out as previously described (6). In brief, nuclear protein extracts ($5\ \mu\text{g}$) were incubated with [γ -³²P]ATP-radiolabeled double-stranded oligonucleotides. Chromatin immunoprecipitation (ChIP) assays were carried out as previously described (45) with $5\ \mu\text{g}$ of anti-Sp1 antibody (Santa Cruz Biotech, Santa Cruz, CA) and rabbit pre-immune serum. To detect VEGF mRNA expression, RNA was extracted from cells using Trizol (Invitrogen, Carlsbad, CA) and then cDNA was amplified using reverse transcriptase. VEGF mRNA was amplified by general PCR. Primers are the follows: F: 5'-TGC CTT GCT GCT CTA CCT CC-3'; R: 5'-TCA CCG CCT CGG CTT GTC AC-3'. Primers for GAPDH used for loading control are the follows: F: 5'-GGT ATC GTG GAA GGA CTC AT-3'; R: 5'-ACC ACC TGG TGC TCA GTG TA-3'.

Western Blot and Immunoprecipitation

$50\ \mu\text{g}$ of protein from cells lysed with RIPA buffer was loaded onto 8–12% SDS-gel, transferred to PVDF membrane, and incubated with the appropriate antibodies. Phosphorylated form of c-Src was detected using anti-c-Src pY416 antibody (Cell Signaling, Danvers, MA). To examine FAK phosphorylation, anti-FAK Y397 and anti-FAK Y576/577 (Cell Signaling, Danvers, MA) were used. Antibodies for JNK, pJNK, pERK, ERK, pp38, p38, VEGF, and Actin were purchased from Santa Cruz Biotech (Santa Cruz, CA). For the Rho GTPases activity, substrates such as GST-PAK PBD or GST-Rhotekin RBD induced in *E. coli* were pulled down, incubated with GST-Sepharose beads, and then mixed with $500\ \mu\text{g}$ whole protein. To detect active Rho GTPases, the appropriate antibody such as anti-RhoA (Santa Cruz Biotech, Santa Cruz, CA), anti-Cdc42 (Santa Cruz Biotech, Santa Cruz, CA), or anti-Rac1 (Santa Cruz Biotech, Santa Cruz, CA) was used. Substrate-bound Rho GTPases present their active state.

Statistics

Statistic results in vitro and in vivo were calculated using the standard 2-tailed Students t test on Microsoft Excel. Some statistical analyses of data were performed using the 2-way ANOVA followed by Bonferroni post hoc test using the GraphPad Quickcalc online web site (<http://www.graphpad.com/quickcalcs/postest1.cfm>).

Results

Kp-10 inhibits HUVEC migration, invasion, and tube formation

To understand the function of Kp-10 in HUVECs, we examined the expression of GPR54, the endogenous receptor for Kp-10 in different cell lines. Our data indicate that GPR54 is

expressed in HUVEC, N3 cells, but not in CHO, Cos7, NIH3T3, and HEK293T cells (Fig. 1A, left). As endothelial cell proliferation is important and necessary for angiogenesis, we investigated the inhibitory effect of Kp-10 on the growth of endothelial cells. Survival curves obtained with the MTS assay showed that high concentration of Kp-10 did not inhibit the proliferation of HUVECs (Fig. 1A, right), suggesting that Kp-10 has little effect on HUVEC proliferation at normal physiological concentration. As cell migration and invasion are two key steps for endothelial cells to form new blood vessels during angiogenesis processes, we performed wound-healing and Boyden chamber migration and invasion assays to determine the effects of Kp-10 on HUVEC migration and invasion. Kp-10 inhibited the migration of HUVECs in a dose dependent manner (Fig. 1B and 1C). *In vitro*, endothelial cells can spontaneously form a three-dimensional tubular capillary-like network on matrigel culture. To examine the effect of Kp-10 on HUVEC tubule formation, we performed the tubule formation assays in the presence of different concentrations of Kp-10 peptide in matrigel. As shown in figure 1D, Kp-10 dramatically inhibited HUVEC tube formation in a dose-dependent manner, suggesting that Kp-10 regulate angiogenesis *in vitro*.

The concentration of Kp-10 used in the angiogenesis study with HUVEC is much higher than that used in standard intracellular Ca^{2+} measurement. To make sure that Kp-10 used in our assay conditions are active, we performed intracellular Ca^{2+} measurement in both CHO cells overexpressing GPR54 and HUVECs (endogenous GPR54). Our data indicate that Kp-10 activates intracellular Ca^{2+} in CHO-GPR54 cells with a EC_{50} at 23 nM while the EC_{50} is about 225 nM in HUVECs (Fig. S1). These data indicate that Kp-10 is active and the effect of Kp-10 in HUVEC requires much higher concentration, which is similar to the effects we observed for Kp-10 in the inhibition of HUVEC angiogenic abilities.

Kp-10 suppresses angiogenesis *in vivo*

To determine the effects of Kp-10 on angiogenesis *in vivo*, we examined whether Kp-10 regulates angiogenesis using the chorioallantoic membrane (CAM) assays. As shown in figure 2A, Kp-10 inhibited chicken embryonic blood vessel formation at the concentration of 5–20 μg per disk. Within avascular areas (the circle area of 15 mm diameter with about 176 mm^2 around a filter paper disk), the number of newly-formed blood vessels (black arrows) was significantly decreased in Kp-10 treated disk (Fig. 2A, left). The effect of Kp-10 is dose-dependent without any inflammation (Fig. 2A, right). These data suggest that Kp-10 suppresses angiogenesis in chicken embryonic blood vessel formation assays.

To confirm the anti-angiogenic activity of Kp-10 in CAM assays, we further performed mouse corneal micropocket assay (Fig. 2B). Micropellets (pointed with arrows) coated with the slow release polymer-hydrogel containing control buffer, VEGF, Kp-10, or VEGF and Kp-10 were implanted into the avascular corneas of C57BL/6 mice, respectively. VEGF strongly induce new blood vessel formation in mouse cornea (Fig. 2B, VEGF, left). Addition of 10 μg Kp-10 significantly inhibited VEGF-induced neovascularization in the cornea (Fig. 2B, VEGF+Kp-10, right). Quantitation of corneal neovascularization, presented as vessel length, clock hour (the proportion of the circumference vascularized when the eye is viewed as a clock), and vessel area, showed that Kp-10 blocked VEGF-induced corneal neovascularization by 60–80% (Fig. 2C). As for the controls, we have used PBS, a scrambled peptide, and the Kp-10 lacking the C-terminal amide in the experiments, the scrambled peptide has no effect on angiogenesis while the Kp-10 without C-terminal amide has weak effect on angiogenesis at similar concentration in the assay (data not shown). In all treated mouse corneal experiments, no inflammation was observed and no weight loss or unusual behavior was detected, suggesting that Kp-10 has no or very little toxicity at the described experimental doses. These results suggest that Kp-10 significantly inhibits VEGF-induced angiogenesis *in vivo*.

Kp-10 inhibits tumor angiogenesis and tumor growth

To understand whether Kp-10 directly affects tumor cell growth, we performed PC-3 cancer cell proliferation assay. As shown in figure 3A, Kp-10 has little effect on tumor cell proliferation *in vitro* even at high concentration (100 μ M) ($p>0.05$), suggesting that Kp-10 had no direct effect on tumor cell proliferation. Given that tumor growth is angiogenesis dependent and suppression of angiogenesis can inhibit tumor growth, we further examined the inhibitory function of tumor growth by Kp-10 using mouse xenograft model. As shown in figure 3B and 3C, after a 45-day treatment with Kp-10, the mean tumor volume of Kp-10-treated group were much less than that of PBS-treated control group ($p<0.01$). In addition, there was little difference in body weight between control and Kp-10-treated mouse groups (Fig. 3C, right), suggesting little side effect of Kp-10 in the mouse model. To verify the inhibitory effect of Kp-10 on tumor angiogenesis, we stained the 5 μ m tumor sections with anti-CD31 antibody. The average vessel number in Kp-10-treated group was dramatically less than that in tumors of control group (Fig. 3D), indicating that Kp-10 significantly inhibits tumor angiogenesis and prevents tumor growth.

Kp-10 decreases Sp1-dependent VEGF expression

As the expression level of VEGF is important for tumor angiogenesis (3–5), we examined whether Kp-10 affects VEGF expression. As shown in figure 4A, Kp-10 decreased expression of both VEGF mRNA and protein in HUVEC. Thus, we further investigated whether Kp-10 regulated VEGF promoter activity in certain conditions such as hypoxia. As shown in figure 4B, Kp-10 not only suppressed the basal VEGF promoter activity but also decreased the activity of VEGF promoter (pVEGF₂₀₁₈-luc) in both hypoxia (CoCl₂-treated cells) and HIF1 α -overexpressing cells, respectively (Fig. 4B, left). Since the VEGF promoter contains both HIF1 α (hypoxia inducing factor α) binding region and the GC-rich region for Sp1 binding, we next examined whether or not the regulation of VEGF promoter activity by Kp-10 is dependent on hypoxia stimulation. Using the two luciferase-reporting vectors containing the GC-rich regions where the HIF1 α -binding site is deleted (pVEGF₁₃₃-luc or pVEGF₈₅-luc), we demonstrate that Kp-10 significantly inhibited the activity of VEGF promoter (Fig. 4B, right), suggesting that Kp-10 regulate the expression of VEGF in an HIF1 α -independent manner.

As VEGF promoter contains high GC boxes to which Sp1 binds (8–11), we examined whether Kp-10 affected VEGF promoter binding of Sp1 using EMSA and ChIP assays. As shown in figure 4C, Kp-10 at 1 μ M inhibited DNA binding of Sp1 to the VEGF promoter in EMSA assay in both hypoxia and normal conditions (with or without the treatment of CoCl₂). To further confirm the effect of Kp-10 on Sp1 binding of VEGF promoter, we perform ChIP assays using different concentrations of Kp-10 in the treatment (Fig. 4D). Our data demonstrated that Kp-10 inhibited the binding activity of Sp1 protein to VEGF promoter and suppress Sp1-dependent VEGF expression in endothelial cells.

Kp-10 down-regulates FAK- and Rac1/Cdc42-mediated migration signaling pathway in the endothelial cells

We next analyzed Kp-10-inhibitory signaling pathways against VEGF-induced HUVEC migration during the processes of tumor angiogenesis. Upon VEGF stimulation, c-Src is phosphorylated and then interacts with FAK, which follows the activation of molecules downstream of c-Src/FAK complex. Thus, we examined whether Kp-10 affects VEGF-induced activation of c-Src/FAK complex. As shown in figure 5A, Kp-10 decreased VEGF-induced phosphorylation of c-Src at Y416 and inhibited c-Src-mediated phosphorylation of FAK at Y576/577 while Kp-10 has little effect on FAK autophosphorylation at Y397 (Fig. 5A).

To understand how Kp-10 regulates the downstream signaling molecules in HUVEC migration and invasion, we examine the activation of Rho GTPases, key molecular regulators in cell migration and invasion. As shown in figure 5B, Kp-10 inhibits the activation of Rac1 and Cdc42 by decreasing the amount of GTP-bound active forms of Rac1 and Cdc42 as measured in our pull-down assays. On the other hand, Kp-10 increased the activation of RhoA in a dose-dependent manner (Fig. 5B), suggesting that Kp-10 differentially regulate the activation of Rho family of GTPases. In addition, Kp-10 inhibited the phosphorylation of JNK, but not ERK and p38 (Fig. 5C). Together, our data demonstrate that c-Src-mediated FAK phosphorylation and Rho GTPases are targets for Kp-10 inhibition of HUVEC migration and invasion.

Discussion

Previous reports showed that Kp-10 plays a role as vasoconstrictor, causing the narrowing of blood vessels. It is, however, unclear whether Kp-10 affects normal angiogenesis and tumor angiogenesis. In this study, we provide evidence that Kp-10 inhibits angiogenesis and tumor growth via blocking Sp1-dependent VEGF expression and suppressing VEGF-dependent FAK and Rac1/Cdc42 activation.

Angiogenesis is a complex multi-step process that involves cell proliferation, migration, and tube formation. It has been shown that suppression at any step of the processes in angiogenesis will inhibit the formation of new blood vessels (46). In the present paper, we show that Kp-10 significantly inhibits HUVEC migration, invasion, and tube formation, but not proliferation (Fig. 1). Furthermore, Kp-10 inhibited angiogenesis *in vivo* using CAM and mouse corneal micropocket assays (Fig. 2), suggesting that Kp-10 inhibit angiogenesis both *in vitro* and *in vivo*.

The Kp-10 concentration required to inhibit angiogenesis properties are much higher than that used in our intracellular Ca^{2+} signaling assays. Although we do not know the exact reasons for the much higher concentration of Kp-10 required for the inhibition of angiogenesis, the expression level of endogenous expressed GPR54 in HUVECs is much lower than that in CHO cells overexpressing GPR54 in our Ca^{2+} measurement experiments and in the literatures. In addition, HUVECs are large vessel endothelium, which makes them suboptimal for angiogenesis studies. Therefore, higher concentration of Kp-10 is required for inhibiting tumor angiogenesis while lower concentration of Kp-10 can induce intracellular Ca^{2+} signaling pathway and have its normal physiological functions in puberty.

Since tumor growth and metastasis depend on tumor angiogenesis, inhibition of tumor angiogenesis is a novel therapeutic modality towards controlling tumor metastasis (47). Kp-10 significantly inhibited the angiogenic tumor growth (Fig. 3B, and 3C) but had little effect on tumor cell proliferation *in vitro* (Fig. 3A), suggesting that Kp-10 inhibits tumor growth not directly through inhibiting tumor cell proliferation *per se* but through inhibiting tumor angiogenesis. In addition, Kp-10-treated mice did not show any body weight loss compared to cisplatin-treated tumor-bearing mice, suggesting that Kp-10 has little toxicity as compared to traditional anti-tumor drugs.

VEGF plays a key role in physiological blood vessel formation and pathological angiogenesis. In our studies, we demonstrate that Kp-10 inhibits Sp1-mediated VEGF expression in endothelial cells independently of the hypoxia condition (Fig. 4), suggesting that Kp-10 could block the initiation step of tumor angiogenesis by regulating the expression level of VEGF. Furthermore, Kp-10 inhibited endothelial cell migration and invasion via VEGF-mediated signaling, suggesting that Kp-10 targets multiple steps of tumor angiogenesis (Fig. 6).

In endothelial cells, VEGF activates c-Src and FAK, subsequently, the formation of c-Src/FAK signaling complex. Our data demonstrated that Kp-10 inhibited VEGF-induced phosphorylation of FAK (Fig. 5A). However, Kp-10 did not affect VEGFR phosphorylation (data not shown). Thus, Kp-10 via GPR54 appears to target VEGFR-induced activation of FAK in endothelial cells (Fig. 6). In addition, Kp-10 inhibits the activation of Rac1 and Cdc42 GTPases and JNK in the cells (Fig. 5B and 5C), indicating that Kp-10 inhibits key signaling molecules in cell migration and invasion (48–50) (Fig. 6).

In conclusion, our data show that Kp-10 inhibits angiogenesis and suppresses tumor growth *in vivo* through inhibiting tumor angiogenesis by selectively blocking Sp1-dependent VEGF expression and by suppressing VEGF-mediated FAK and Rac1/Cdc42 activation in endothelial cells (Fig. 6). Our new finding of Kp-10 function in angiogenesis suggests a new role of kisspeptins as an anti-angiogenesis agent.

Acknowledgments

This study is partially supported by a grant from National Cancer Institute (NIH) 1R01CA106479 to M Liu, and by the Research Platform of Cell Signaling Networks from the Science and Technology Commission of Shanghai Municipality (06DZ22923). We thank Dr. Xin-li Wang at Baylor College of Medicine for the HUVECs used in our studies.

References

1. Yi T, Yi Z, Cho SG, et al. Gambogic acid inhibits angiogenesis and prostate tumor growth by suppressing vascular endothelial growth factor receptor 2 signaling. *Cancer research*. 2008; 68(6): 1843–50. [PubMed: 18339865]
2. Bhat TA, Singh RP. Tumor angiogenesis - A potential target in cancer chemoprevention. *Food Chem Toxicol*. 2007
3. Breen EC. VEGF in biological control. *J Cell Biochem*. 2007; 102(6):1358–67. [PubMed: 17979153]
4. Nagy JA, Dvorak AM, Dvorak HF. VEGF-A and the Induction of Pathological Angiogenesis. *Annu Rev Pathol*. 2007; 2:251–75. [PubMed: 18039100]
5. Barr MP, Bouchier-Hayes DJ, Harme J. Vascular endothelial growth factor is an autocrine survival factor for breast tumour cells under hypoxia. *Int J Oncol*. 2008; 32(1):41–8. [PubMed: 18097541]
6. Schafer G, Cramer T, Suske G, Kemmner W, Wiedenmann B, Hocker M. Oxidative stress regulates vascular endothelial growth factor-A gene transcription through Sp1- and Sp3-dependent activation of two proximal GC-rich promoter elements. *The Journal of biological chemistry*. 2003; 278(10): 8190–8. [PubMed: 12509426]
7. Abdelrahim M, Smith R 3rd, Burghardt R, Safe S. Role of Sp proteins in regulation of vascular endothelial growth factor expression and proliferation of pancreatic cancer cells. *Cancer Res*. 2004; 64(18):6740–9. [PubMed: 15374992]
8. Finkenzeller G, Sparacio A, Technau A, Marme D, Siemeister G. Sp1 recognition sites in the proximal promoter of the human vascular endothelial growth factor gene are essential for platelet-derived growth factor-induced gene expression. *Oncogene*. 1997; 15(6):669–76. [PubMed: 9264407]
9. Pore N, Liu S, Shu HK, et al. Sp1 is involved in Akt-mediated induction of VEGF expression through an HIF-1-independent mechanism. *Mol Biol Cell*. 2004; 15(11):4841–53. [PubMed: 15342781]
10. Shi Q, Le X, Abbruzzese JL, et al. Constitutive Sp1 activity is essential for differential constitutive expression of vascular endothelial growth factor in human pancreatic adenocarcinoma. *Cancer Res*. 2001; 61(10):4143–54. [PubMed: 11358838]
11. Zhang J, Jia Z, Li Q, et al. Elevated expression of vascular endothelial growth factor correlates with increased angiogenesis and decreased progression-free survival among patients with low-grade neuroendocrine tumors. *Cancer*. 2007; 109(8):1478–86. [PubMed: 17340592]

12. Rudge JS, Holash J, Hylton D, et al. Inaugural Article: VEGF Trap complex formation measures production rates of VEGF, providing a biomarker for predicting efficacious angiogenic blockade. *Proc Natl Acad Sci U S A*. 2007; 104(47):18363–70. [PubMed: 18000042]
13. Li D, Yu W, Liu M. Regulation of KiSS1 gene expression. *Peptides*. 2008
14. Kotani M, Detheux M, Vandenberghe A, et al. The metastasis suppressor gene KiSS-1 encodes kisspeptins, the natural ligands of the orphan G protein-coupled receptor GPR54. *J Biol Chem*. 2001; 276(37):34631–6. [PubMed: 11457843]
15. Ohtaki T, Shintani Y, Honda S, et al. Metastasis suppressor gene KiSS-1 encodes peptide ligand of a G-protein-coupled receptor. *Nature*. 2001; 411(6837):613–7. [PubMed: 11385580]
16. Lee JH, Miele ME, Hicks DJ, et al. KiSS-1, a novel human malignant melanoma metastasis-suppressor gene. *Journal of the National Cancer Institute*. 1996; 88(23):1731–7. [PubMed: 8944003]
17. Lee JH, Welch DR. Suppression of metastasis in human breast carcinoma MDA-MB-435 cells after transfection with the metastasis suppressor gene, KiSS-1. *Cancer Res*. 1997; 57(12):2384–7. [PubMed: 9192814]
18. Stafford LJ, Xia C, Ma W, Cai Y, Liu M. Identification and characterization of mouse metastasis-suppressor KiSS1 and its G-protein-coupled receptor. *Cancer research*. 2002; 62(19):5399–404. [PubMed: 12359743]
19. Sanchez-Carbayo M, Capodiceci P, Cordon-Cardo C. Tumor suppressor role of KiSS-1 in bladder cancer: loss of KiSS-1 expression is associated with bladder cancer progression and clinical outcome. *The American journal of pathology*. 2003; 162(2):609–17. [PubMed: 12547718]
20. Dittmer A, Vetter M, Schunke D, et al. Parathyroid hormone-related protein regulates tumor-relevant genes in breast cancer cells. *The Journal of biological chemistry*. 2006; 281(21):14563–72. [PubMed: 16551631]
21. Jiang T, Zhang SL, Lin B, Meng LR, Gao H. Expression and clinical significance of KISS-1 and GPR54 mRNA in endometrial carcinoma. *Zhonghua Zhong Liu Za Zhi*. 2005; 27(4):229–31. [PubMed: 15949424]
22. Nicolle G, Comperat E, Nicolaiew N, Cancel-Tassin G, Cussenot O. Metastin (KISS-1) and metastin-coupled receptor (GPR54) expression in transitional cell carcinoma of the bladder. *Ann Oncol*. 2007; 18(3):605–7. [PubMed: 17164231]
23. Sanchez-Carbayo M, Belbin TJ, Scotlandi K, et al. Expression profiling of osteosarcoma cells transfected with MDR1 and NEO genes: regulation of cell adhesion, apoptosis, and tumor suppression-related genes. *Lab Invest*. 2003; 83(4):507–17. [PubMed: 12695554]
24. Nash KT, Phadke PA, Navenot JM, et al. Requirement of KISS1 secretion for multiple organ metastasis suppression and maintenance of tumor dormancy. *Journal of the National Cancer Institute*. 2007; 99(4):309–21. [PubMed: 17312308]
25. Ohta S, Lai EW, Pang AL, et al. Downregulation of metastasis suppressor genes in malignant pheochromocytoma. *Int J Cancer*. 2005; 114(1):139–43. [PubMed: 15523699]
26. Ikeguchi M, Yamaguchi K, Kaibara N. Clinical significance of the loss of KiSS-1 and orphan G-protein-coupled receptor (hOT7T175) gene expression in esophageal squamous cell carcinoma. *Clin Cancer Res*. 2004; 10(4):1379–83. [PubMed: 14977840]
27. Jiang Y, Berk M, Singh LS, et al. KiSS1 suppresses metastasis in human ovarian cancer via inhibition of protein kinase C alpha. *Clin Exp Metastasis*. 2005; 22(5):369–76. [PubMed: 16283480]
28. Dhar DK, Naora H, Kubota H, et al. Downregulation of KiSS-1 expression is responsible for tumor invasion and worse prognosis in gastric carcinoma. *Int J Cancer*. 2004; 111(6):868–72. [PubMed: 15300798]
29. Masui T, Doi R, Mori T, et al. Metastin and its variant forms suppress migration of pancreatic cancer cells. *Biochem Biophys Res Commun*. 2004; 315(1):85–92. [PubMed: 15013429]
30. Marot D, Bieche I, Aumas C, et al. High tumoral levels of Kiss1 and G-protein-coupled receptor 54 expression are correlated with poor prognosis of estrogen receptor-positive breast tumors. *Endocrine-related cancer*. 2007; 14(3):691–702. [PubMed: 17914099]
31. Martin TA, Watkins G, Jiang WG. KiSS-1 expression in human breast cancer. *Clin Exp Metastasis*. 2005; 22(6):503–11. [PubMed: 16320113]

32. Ikeguchi M, Hirooka Y, Kaibara N. Quantitative reverse transcriptase polymerase chain reaction analysis for KiSS-1 and orphan G-protein-coupled receptor (hOT7T175) gene expression in hepatocellular carcinoma. *J Cancer Res Clin Oncol*. 2003; 129(9):531–5. [PubMed: 12898236]
33. Seminara SB, Messenger S, Chatzidaki EE, et al. The GPR54 gene as a regulator of puberty. *N Engl J Med*. 2003; 349(17):1614–27. [PubMed: 14573733]
34. Zhang C, Roepke TA, Kelly MJ, Ronnekleiv OK. Kisspeptin depolarizes gonadotropin-releasing hormone neurons through activation of TRPC-like cationic channels. *J Neurosci*. 2008; 28(17):4423–34. [PubMed: 18434521]
35. Colledge WH. GPR54 and puberty. *Trends in endocrinology and metabolism: TEM*. 2004; 15(9):448–53. [PubMed: 15519892]
36. Seminara SB, Kaiser UB. New gatekeepers of reproduction: GPR54 and its cognate ligand, KiSS-1. *Endocrinology*. 2005; 146(4):1686–8. [PubMed: 15769900]
37. d'Anglemont de Tassigny X, Fagg LA, Dixon JP, et al. Hypogonadotropic hypogonadism in mice lacking a functional Kiss1 gene. *Proc Natl Acad Sci U S A*. 2007; 104(25):10714–9. [PubMed: 17563351]
38. d'Anglemont de Tassigny X, Fagg LA, Carlton MB, Colledge WH. Kisspeptin can stimulate gonadotropin-releasing hormone (GnRH) release by a direct action at GnRH nerve terminals. *Endocrinology*. 2008; 149(8):3926–32. [PubMed: 18450966]
39. Thompson EL, Patterson M, Murphy KG, et al. Central and peripheral administration of kisspeptin-10 stimulates the hypothalamic-pituitary-gonadal axis. *J Neuroendocrinol*. 2004; 16(10):850–8. [PubMed: 15500545]
40. Bilban M, Ghaffari-Tabrizi N, Hintermann E, et al. Kisspeptin-10, a KiSS-1/metastin-derived decapeptide, is a physiological invasion inhibitor of primary human trophoblasts. *J Cell Sci*. 2004; 117(Pt 8):1319–28. [PubMed: 15020672]
41. Mead EJ, Maguire JJ, Kuc RE, Davenport AP. Kisspeptins are novel potent vasoconstrictors in humans, with a discrete localization of their receptor, G protein-coupled receptor 54, to atherosclerosis-prone vessels. *Endocrinology*. 2007; 148(1):140–7. [PubMed: 17023533]
42. Yi T, Cho SG, Yi Z, et al. Thymoquinone inhibits tumor angiogenesis and tumor growth through suppressing AKT and extracellular signal-regulated kinase signaling pathways. *Mol Cancer Ther*. 2008; 7(7):1789–96. [PubMed: 18644991]
43. Yi ZF, Cho SG, Zhao H, et al. A novel peptide from human apolipoprotein(a) inhibits angiogenesis and tumor growth by targeting c-Src phosphorylation in VEGF-induced human umbilical endothelial cells. *Int J Cancer*. 2008
44. Kenyon BM, Voest EE, Chen CC, Flynn E, Folkman J, D'Amato RJ. A model of angiogenesis in the mouse cornea. *Invest Ophthalmol Vis Sci*. 1996; 37(8):1625–32. [PubMed: 8675406]
45. Mie Lee Y, Kim SH, Kim HS, et al. Inhibition of hypoxia-induced angiogenesis by FK228, a specific histone deacetylase inhibitor, via suppression of HIF-1alpha activity. *Biochemical and biophysical research communications*. 2003; 300(1):241–6. [PubMed: 12480550]
46. Tournaire R, Simon MP, le Noble F, Eichmann A, England P, Pouyssegur J. A short synthetic peptide inhibits signal transduction, migration and angiogenesis mediated by Tie2 receptor. *EMBO Rep*. 2004; 5(3):262–7. [PubMed: 14978510]
47. Kruger EA, Duray PH, Price DK, Pluda JM, Figg WD. Approaches to preclinical screening of antiangiogenic agents. *Semin Oncol*. 2001; 28(6):570–6. [PubMed: 11740811]
48. Takino T, Nakada M, Miyamori H, et al. JSAP1/JIP3 cooperates with focal adhesion kinase to regulate c-Jun N-terminal kinase and cell migration. *The Journal of biological chemistry*. 2005; 280(45):37772–81. [PubMed: 16141199]
49. Hauck CR, Hsia DA, Puente XS, Cheresh DA, Schlaepfer DD. FRNK blocks v-Src-stimulated invasion and experimental metastases without effects on cell motility or growth. *EMBO J*. 2002; 21(23):6289–302. [PubMed: 12456636]
50. Avraham HK, Lee TH, Koh Y, et al. Vascular endothelial growth factor regulates focal adhesion assembly in human brain microvascular endothelial cells through activation of the focal adhesion kinase and related adhesion focal tyrosine kinase. *The Journal of biological chemistry*. 2003; 278(38):36661–8. [PubMed: 12844492]

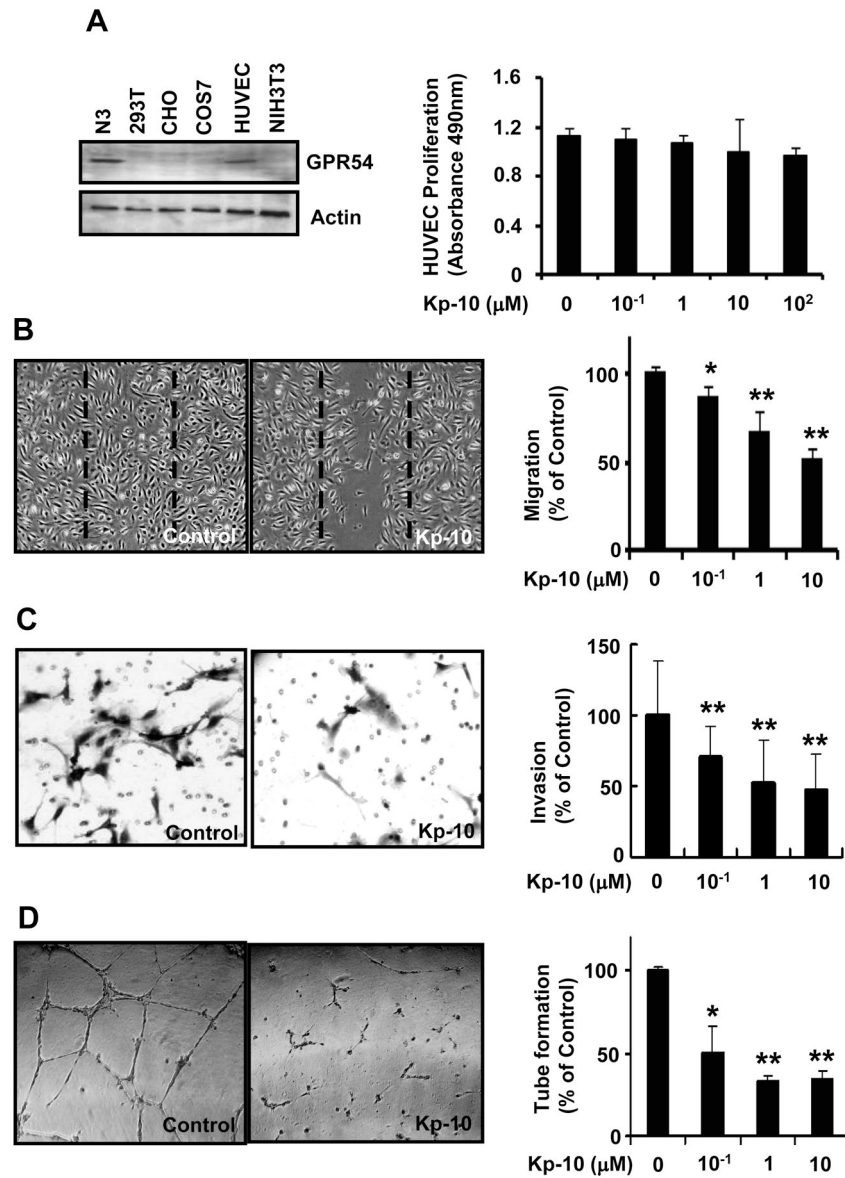


Figure 1. Kp-10 inhibits angiogenic properties of endothelial cells

(A) GPR54 was expressed in HUVEC (left). Using Western blotting, the expression of GPR54 was examined in N3, 293T, CHO, COS7, HUVEC, and NIH3T3 cells. GPR54 was found in hypothalamic N3 cell line and HUVECs. Actin was used for a loading control. Kp-10 has little effect on HUVEC proliferation (Right). 5000 HUVECs were plated at 96-well plate. The cells were treated with different concentration of Kp-10 and then were measured using the CellTiter96 AQueous One solution cell proliferation assay kit (Promega). (B) Kp-10 inhibits HUVEC migration in wound-healing migration assays. HUVECs were plated, scratched, and incubated in medium with 4ng/ml VEGF in the presence or absence of various concentrations of Kp-10 peptide. Kp-10 significantly inhibited the VEGF-induced migration of HUVEC to the wound area. Representative photomicrographs of cells treated with VEGF, and cells treated with VEGF together with Kp-10 were shown. Dotted lines indicate the area occupied by the initial scraping. * $p < 0.05$, ** $p < 0.01$ versus VEGF-treated control. (C) Inhibition of HUVEC invasion by Kp-10

using Boyden chamber migration assays. 4×10^4 cells were placed into the top chamber of Boyden chamber (8 μ m). VEGF was added to the bottom chamber and incubated at 37°C for 4 hours. HUVECs were fixed and then stained with H&E and counted under the microscope. ** $p < 0.01$. (D) Kp-10 inhibited HUVEC tubule formation. Representative photomicrographs of tubule formation in the control and Kp-10-treated groups were shown. About 4×10^4 cells were plated in 24-well plates previously coated with matrigel, and incubated for 16 hours at 37°C in the absence or presence of Kp-10 (right). Tubular structures were counted. 'Percentage (%) of control' is the mean number of tubules expressed as a proportion of that in the control group. *, $p < 0.05$; **, $p < 0.01$.

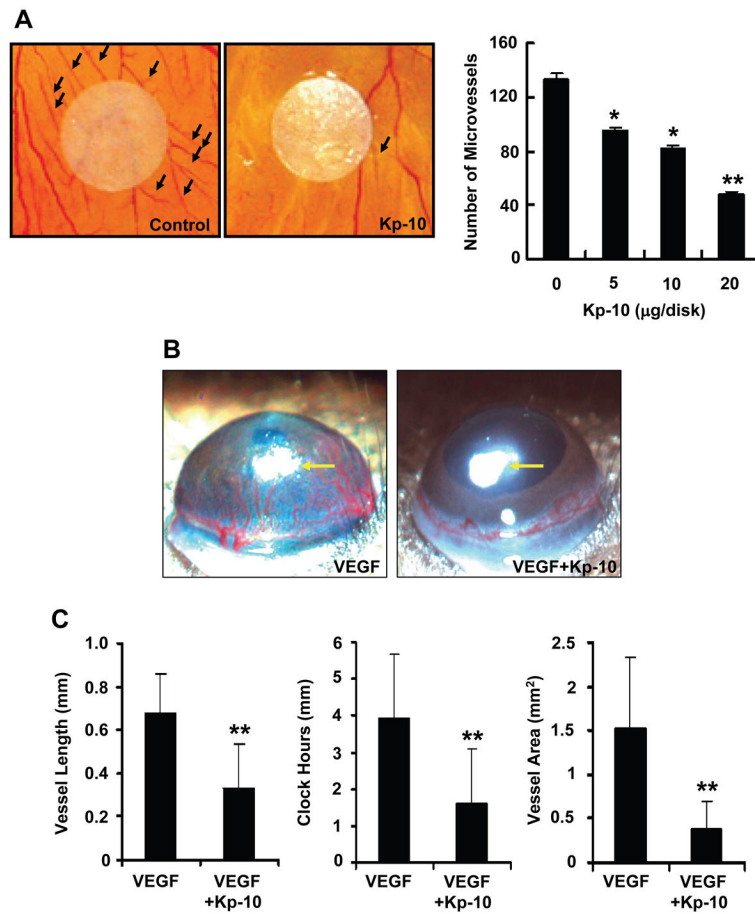


Figure 2. Inhibition of angiogenesis by Kp-10 *in vivo*

(A) Kp-10 inhibits angiogenesis in chicken embryo chorioallantoic membrane (CAM) assay. Representative pictures of PBS-control and Kp-10-treated CAM, showing inhibition of new blood vessel growth (black arrows) by the treatment of different concentrations of Kp-10 within a defined area surrounding the implanted disk. *, $p < 0.05$ and **, $p < 0.01$. (B) Kp-10 inhibits angiogenesis using mouse corneal micropocket assay. Micropellets (yellow arrows) containing 160 ng of VEGF were implanted into corneal micropockets of C57BL/6 mice as described in materials and methods. The effects of Kp-10 on angiogenesis *in vivo* were examined using slow-releasing polymer containing four different treatment groups: saline alone, 1 µg Kp-10 alone, 160 ng VEGF alone, and 160 ng VEGF plus 1 µg Kp-10. Saline alone and Kp-10 alone were used as controls in the experiments. Corneal neovascularization was measured and photographed with a stereo-microscope on day 7 after implantation. Positions of pellets were pointed with arrows. (C) Kp-10 inhibited vessel length, clock hours of circumferential neovascularization, and the area of neovascularization, respectively. The bio-microscopic assessment was conducted by two independent observers. Results are given as mean ± SEM. **, $p < 0.01$.

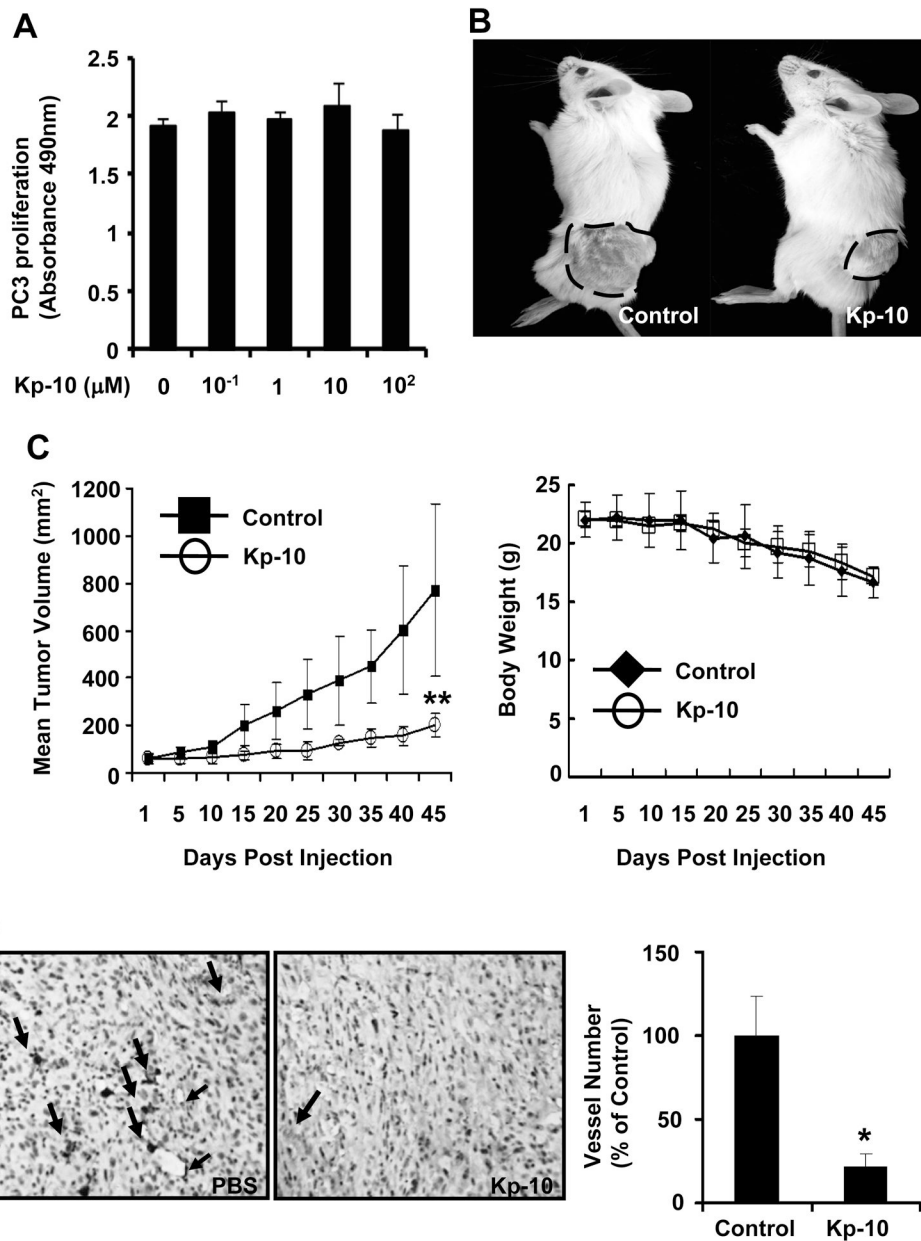


Figure 3. Kp-10 inhibits tumor growth and tumor angiogenesis in xenograft mice
 (A) Kp-10 has little effect on tumor cell (PC-3) proliferation with 100 μM Kp-10 using Cell Titer96 AQueous One solution cell proliferation assay. (B) Treatment of Kp-10 inhibited tumor growth. Typical example of tumor-bearing mice of the PBS control (left) or Kp-10-treated groups (right) on day 45. Tumor was marked with a dot line. (C) Quantitative analysis of tumor volumes between PBS-treated and Kp-10-treated tumor and quantitative analysis of the mouse body weight between PBS-treated and Kp-10-treated mice during the treatment period. The tumor volume data are presented as mean ± SD (**, $p < 0.01$). (D) Effects of Kp-10 on tumor angiogenesis in xenograft mouse tumor model. Tumors were fixed and embedded with paraffin. The 5 μm sections were stained with CD31 antibody. The average vessel number in tumors of control group was significantly more than that of Kp-10 treatment group (*, $p < 0.05$).

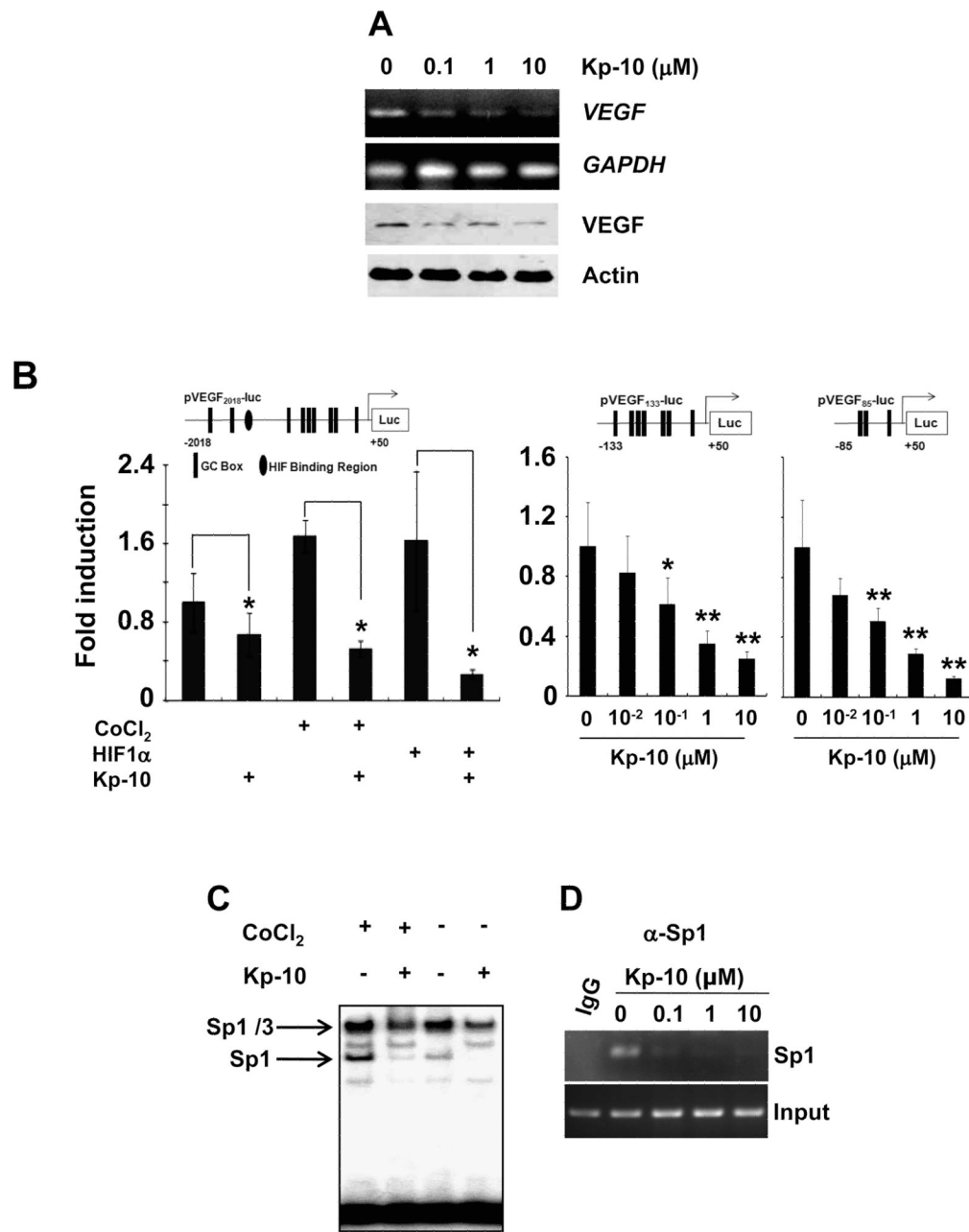


Figure 4. Kp-10 decreases Sp1-dependent VEGF expression

(A) Kp-10 inhibits VEGF expression in HUVECs. HUVECs were treated with different concentrations of Kp-10 for 24hrs and then subjected to RT-PCR and Western blot analysis with anti-VEGF antibody. GAPDH and actin were used for PCR and Western blot loading controls, respectively. (B) Kp-10 mediates the inhibitory effect through the GC-rich boxes in VEGF-promoter regions. (Left) HUVEC transfected with pVEGF₂₀₁₈-luc was treated with CoCl₂ or HIF1 α in the presence or absence of 1 μM of Kp-10. At 24hr, luciferase assays were performed. *, *p*<0.05. (Middle and right) HUVEC was transfected with pVEGF₁₃₃-luc or pVEGF₈₅-luc plasmid, and then treated with different concentrations of Kp-10 (10⁻², 10⁻¹, 1, and 10 μM) for 24hrs before luciferase activity was examined. *, *p*<0.05; **, *p*<0.01. (C) Kp-10 inhibits the DNA binding activity of Sp1 protein to VEGF promoter

region in EMSA assays. Kp-10 inhibits both hypoxia-independent and dependent Sp1 DNA-binding activity to VEGF promoter. When HUVEC was exposed to 1 μ M of Kp-10 for 24hr, the binding of Sp1 to VEGF promoter region was diminished. The effects of Kp-10 on Sp1 DNA binding of VEGF promoter in hypoxic condition were measured with the addition of 100nM of CoCl₂. (D) Kp-10 inhibits DNA binding activity of Sp1 to VEGF promoter *in vivo*. ChIP assays were performed with different concentrations of Kp-10 after the cells were treated for 24 hr.

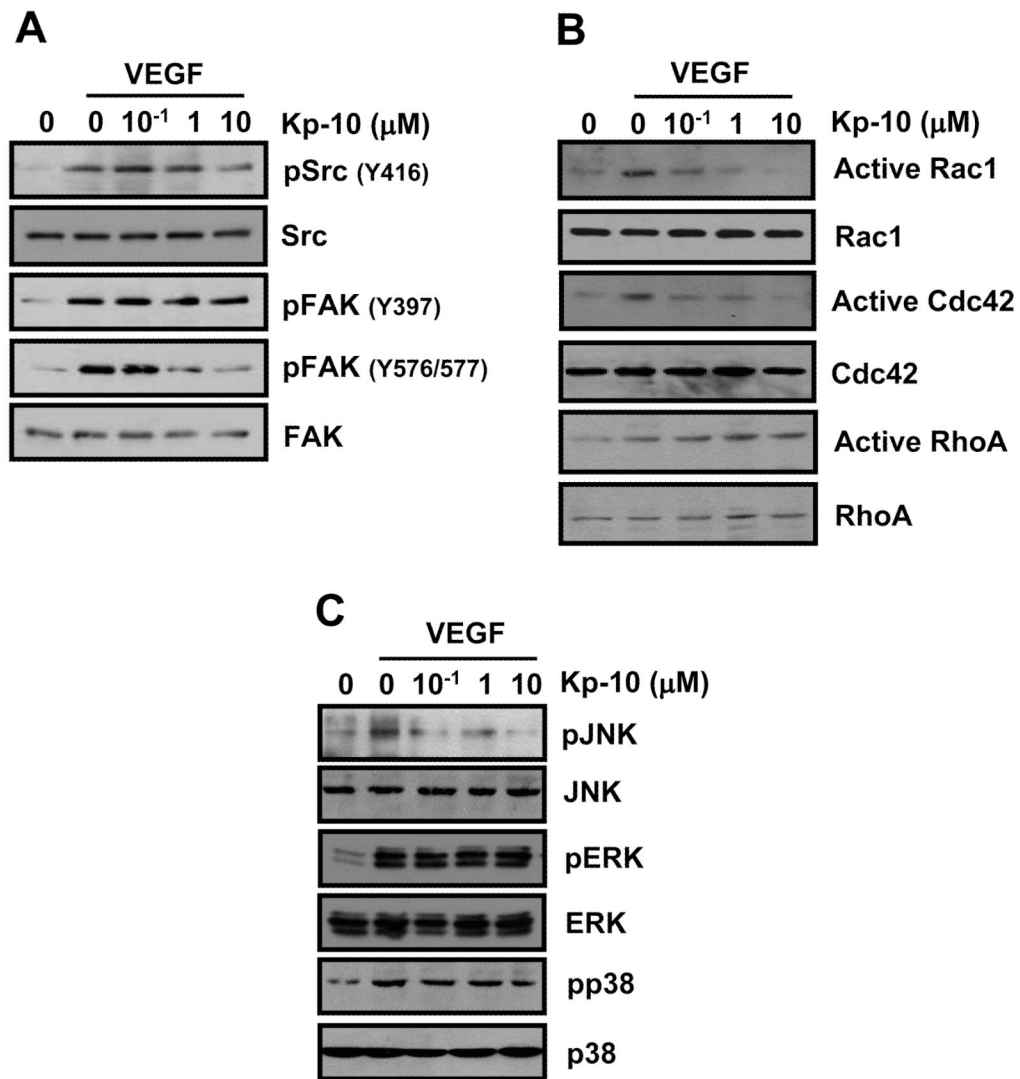


Figure 5. Kp-10 inhibits the phosphorylation of c-Src/FAK and their downstream signaling proteins

(A) Kp-10 decreased VEGF-activated phosphorylation of c-Src and FAK. Cells were treated with VEGF alone or VEGF plus Kp-10 for 5min. VEGF-dependent phosphorylation of c-Src and FAK was detected with anti-Src pY416, anti-FAK pY397, anti-FAK pY576/577 antibody, respectively. (B) Kp-10 down-regulates the activation of Rac1 and Cdc42 (GTP-binding) while activates RhoA in the GTPase pull-down assays. Cells were stimulated with the indicatives for 5min. The activity assays of RhoGTPases were performed using GST-PBD (PAK binding domain) and GST-RBD (Rhotekin binding domain) as previously described in our lab (34). (C) Kp-10 decreased VEGF-induced phosphorylation of JNK while has little effects on the phosphorylation of ERK1/2 and p38 kinases. Phosphorylation of MAPKs was examined using different antibodies as indicated after HUVECs were stimulated with VEGF alone or VEGF plus Kp-10 for 15min.

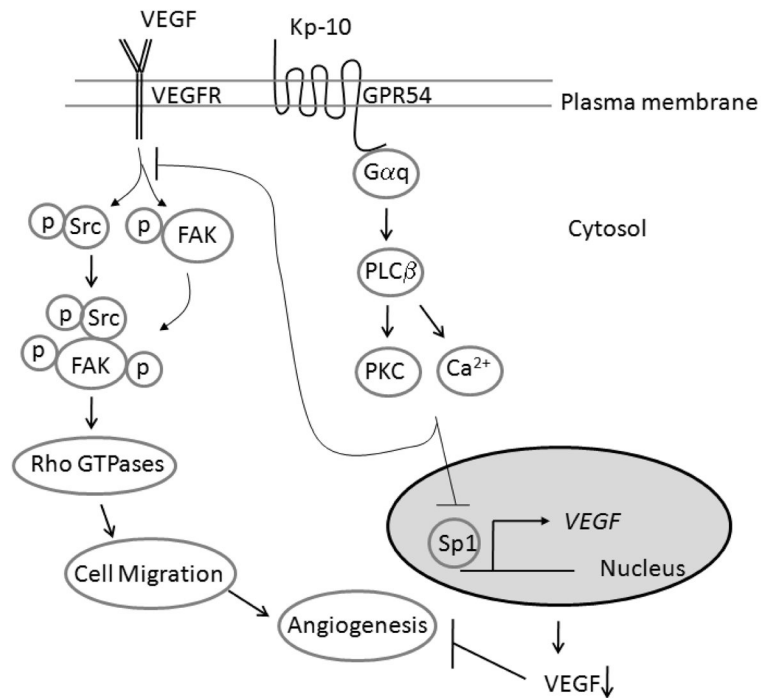


Figure 6. Diagram of Kp-10 mediated inhibition of tumor angiogenesis by suppressing Src/FAK and Rac1/Cdc42 signaling pathways and VEGF expression. Kp-10 activates Gpr54 and Gαq signaling pathways and suppresses Sp1 binding of VEGF promoter and VEGF expression. At the same time, Kp-10 activated GPR54-G-protein signaling axis regulates the phosphorylation and activation of Src and FAK as well as RhoGTPases (Rac1 and Cdc42), leading to the inhibition of cell migration and invasion. Down regulation of VEGF expression and suppression of cell migration and invasion by addition of Kp-10 peptide leads to the inhibition of angiogenesis. Therefore, Kp-10 inhibits angiogenesis by suppressing Src-mediated FAK and Rac/Cdc42 signaling pathways and the expression of VEGF.